DOI: 10.1002/ejic.200900298

Substituent Effects on Structural, Electronic, and Redox Properties of Bis(*N*-alkyl-2-oxy-1-naphthaldiminato)copper(II) Complexes Revisited – Inequivalence in Solid- and Solution-State Structures by Electronic Spectroscopy and X-ray Diffraction Explained by DFT

Manuel Villagrán,[a] Francesco Caruso,[b][‡] Miriam Rossi,[c] José H. Zagal,[a] and Juan Costamagna*[a][‡]

Keywords: Naphthaldiminate ligands / Stereochemistry / Cyclic voltammetry / Copper / Substituent effects / Density functional calculations

Bis(*N*-alkyl-2-oxy-1-naphthaldiminato)copper(II) complexes in the solid state and in *N*,*N*′-dimethylformamide (DMF) solutions were studied by electronic spectroscopy, X-ray diffraction, DFT calculations, and cyclic voltammetry. The established correlation between the bulkiness of the imine nitrogen substituent, deformation of the copper coordination sphere, and the Cu^{II}/Cu^{I} couple potential in DMF solutions has been re-evaluated, and its inconsistencies explained by using results from DFT calculations and spectroscopic data. According to these DFT calculations, the coordination sphere of the *N*-ethyl derivative has a flat-tetrahedral geometry. The N–Cu–N′ and O–Cu–O′ angles and the dihedral angle between the planes N–Cu–O and N′–Cu–O′ in the solid state found by X-ray diffraction in this study are affected by crystal packing forces. UV/Vis spectra of the *N*-ethyl, *N*-*i*Pr, and *N*-*t*Bu derivatives suggest that the first two compounds have fluxional behavior characterized by a centrosymmetric transition state, whereas the *t*Bu group in the *N*-*t*Bu derivative prevents such dynamic action. In the crystal, this *N*-*t*Bu complex changes upon DFT geometry optimization to a more tetrahedral configuration. Therefore, in contrast to X-ray crystal structures reported in the literature of complexes with primary *N*-alkyl substituents that show a planar Cu coordination sphere (i.e. N–Cu–N′ and O–Cu–O′ bond angles of 180°), these complexes are not planar in solution or as isolated molecules.

Introduction

The synthesis and electrochemical characterization of Schiff base complexes is a subject of current interest because of their structural, magnetic, spectroscopic, catalytic, and redox properties; they are used as models for metalloenzymes, among other areas.[1–7] Previous studies on copper(II) complexes coordinated with Schiff base ligands, both in the solid state and in solution with several solvents, suggested that bulky groups on the imino nitrogen induce distortion about the copper atoms from a planar towards a pseudo-tetrahedral environment, also described as a flat-tetrahedral environment.[2–8] A relationship between the d–d charge-transfer band, observed in the electronic spectra, and the Cu^{II}/Cu^{I} couple reduction potential was established for related compounds.[2c] In addition, Taylor et al. correlated the metrical parameters of the unsubstituted tetradentate copper(II) Schiff base complexes containing N_2O_2, N_2N_2, and N_2S_2 donor moieties with their respective redox potentials.[9] They then studied the impact of the geometric parameters on the redox potential of blue copper proteins by using copper(I) Schiff base complexes derived from *o*-*tert*-butylthiobenzaldehyde and a series of terminal diamines as synthetic models for blue copper proteins;[9c] they found that for a type I copper center, the greatest effect on the operating potential of the protein arises from the Cu–N and Cu–S distances. In the analysis of copper proteins, the more subtle contributions of the geometric parameters (bond angles and geometric flexibility) and the effect of the dielectric strength of the metal-binding pocket are more difficult to assess, because it is not easy to decouple the effect of the many variables present in these species. In model compounds, the influencing factors in these species are decoupled, and, therefore, through the preparation of model compounds and the analysis of their structural and electrochemical properties, Taylor et al. were able to observe a general increase in the oxidation potentials as the geometry changes from planar to tetrahedral in donor and

[a] Facultad de Química y Biología, Universidad de Santiago de Chile,
P. O. B. 40, Santiago 33, Chile
E-mail: juan.costamagna@usach.cl
[b] Istituto di Chimica Biomolecolare, Consiglio Nazionale delle Ricerche,
c/o Universitá di Roma "La Sapienza" Vecchio Istituto Chimico,
P.le Aldo Moro 5, 00185 Rome, Italy
[c] Vassar College, Department of Chemistry,
Poughkeespie, NY 12604-0484, USA
[‡] J. C. and F. C. contributed equally to this work

nondonor solvents. However, although some rudimentary calculations with respect to the impact of the geometry on the redox potential can be made, by using these data, one must bear in mind that the metrical parameters from X-ray analysis may not be rigorously conserved in solution.

In this work, the crystal structures of bis(*N*-ethyl-2-oxy-1-naphthaldiminato)copper(II) (**2**) and bis(*N*-*tert*-butyl-2-oxy-1-naphthaldiminato)copper(II) (**4**) are reported; these species along with related *N*-methyl (**1**) and *N*-*i*Pr (**3**) complexes are also characterized spectroscopically, electrochemically, and with theoretical calculations. As mentioned above, the relationship between the bulkiness of the substituent on the imine nitrogen atom and the deformation of the copper coordination sphere (Scheme 1) has been described. However, some small bulky groups induce larger distortion from planarity than expected. For instance, in bis(*N*-isopentyl-2-oxy-1-naphthaldiminato)copper(II) and bis(*N*-*sec*-butyl-2-oxy-1-naphthaldiminato)copper(II) complexes, the distortions shown by the dihedral angle between the planes N–Cu–O and N′–Cu–O′ (defined as *Dih*) is 25.7° and 39.5°, respectively (Scheme 1 and later shown in Table 4), i.e. contrary to the larger bulk of the isopentyl group, its complex is less distorted than the *sec*-butyl complex. Another example is the *N*-isopropyl-salicylaldiminate Cu^{II} complex, which has a dihedral angle distortion of 59.7°, almost the same as the corresponding *tert*-butyl derivative (distortion of 61.6°, Table 4). If the coordination sphere was *only* affected by bulkiness of the substituent, the isopropyl derivative would induce a smaller distortion than that caused by the *tert*-butyl derivative. Here, we provide an explanation for such an apparent inconsistency and describe how the potential of the Cu^{II}/Cu^{I} couple in *N*,*N*′-dimethylformamide solutions is affected.

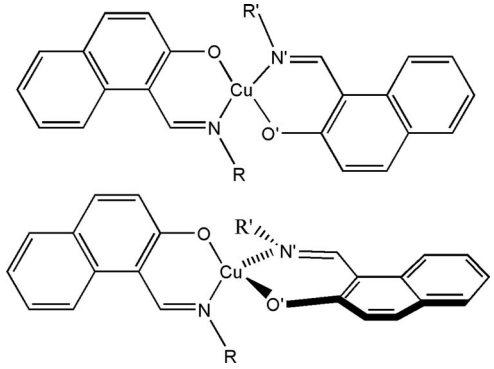

Scheme 1. Planar (top) and flat-tetrahedral (bottom) configurations, which corresponding to *Dih* = 0° and *Dih* ≠ 0°, respectively (*Dih* = dihedral angle between the planes N–Cu–O and N′–Cu–O′; R = R′). Compound **1**: R = methyl, **2**: R = ethyl, **3**: R = *i*Pr, **4**: R = *t*Bu.

Results and Discussion

Spectrochemical and Electrochemical Results

Table 1 contains the electronic spectroscopy results observed for the copper(II) complexes synthesized. The electronic spectrum of bis(*N*-methyl-2-oxy-1-naphthaldiminato)-copper(II) (**1**) in the solid state shows an absorption band at ca. 14800 cm^{-1}, which is indicative of a square-planar species.[10] The spectra of bis(*N*-isopropyl-2-oxy-1-naphthaldiminato)copper(II) (**3**) and bis(*N*-*tert*-butyl-2-oxy-1-naphthaldiminato)copper(II) (**4**) show two d–d bands probably arising from distortion from a planar coordination sphere. These bands are assigned to the electronic transition $^2B_1 \rightarrow {}^2B_2$ (8000–10000 cm^{-1}) and $^2A_2 \rightarrow {}^2B_2$ (10000–16,000 cm^{-1}).[11] This distorted geometry can also be described as a flat-tetrahedral geometry. This distortion may be attributed to steric effects of the alkyl group linked to the imine nitrogen atom in the Schiff base ligands, vide infra.

Table 1. Transitions and the positions of their bands (cm^{-1}) in the electronic spectra of the naphthaldiminate complexes in the solid state.

Compound	d–d	π–π*	π–π*	π–π*
1	14800	25900–26600	31800	32800
2	15500	23500–25100	31300	32500
3	12500–14900	25900	31800	32800
4	10200–14600	26000	31800	32300
5		24300–26000	29400	32400

The electronic spectrum of **1** in DMF solution shows one d–d band that may be associated with a Cu^{II} square-planar geometry. Therefore, this compound roughly seems to have the same configuration in the solid state[12] and in DMF solution, as shown in Table 2. Bis(*N*-isopropyl-2-oxy-1-naphthaldiminato)copper(II) in DMF also shows only one d–d band centered at 15200 cm^{-1}, but this is in contrast with its above-mentioned spectrum in the solid state, which suggests a different situation in solution. Table 2 shows that, in DMF solution, **4** has two d–d bands consistent with a distorted flat-tetrahedral symmetry.

Table 2. Transitions and the positions of their bands (cm^{-1}) in the electronic spectra of bis(*N*-R-2-oxy-1-naphthaldiminato)copper(II) complexes in DMF solution.[a]

Compound	d–d (ε)	π–π*(ε)	π–π*(ε)	π–π*(ε)	π–π*(ε)
1	16500 (135)	25600 (4650)	26600 (5050)	32100 (9150)	32800 (9390)
2	16600 (87)	25600 (4290)	26600 (4600)	32500 (9500)	32800 (9700)
3	15300 (190)	25100 (4370)	26300 (4210)	31800 (9120)	32800 (9170)
4	13900 (250)–21700 (1400)	25000 (4930)	26300 (4010)	31800 (9250)	32800 (9500)

[a] ε = molar extinction coefficient ($L\,M^{-1}\,cm^{-1}$).

For the intraligand charge transfer transitions, it is possible to observe two zones. The first zone presents one n–π band located at 20400 cm^{-1} and is only observed for bis(*N*-isopropyl-2-oxy-1-naphthaldiminato)zinc(II) (**5**),[13] while for the copper(II) complexes two intense bands located between 25000 to 26700 cm^{-1} in DMF solution are found and assigned to a π–π* transition of the imine chromophore (Table 2). In the second zone, two π–π* transitions

are seen between 31700–33300 cm^{-1}; they are assigned to the naphthalene ring for all the copper(II) complexes, see Figure 1.

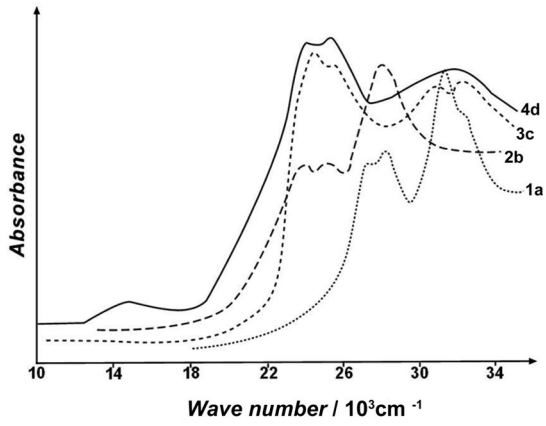

Figure 1. Electronic spectra in DMF solution of a copper(II) Schiff base complex and precursors: a – 2-oxy-1-naphthaldehyde, b – *N*-ethyl-2-oxy-1-naphthaldimine, c – bis(*N*-ethyl-2-oxy-1-naphthaldiminato)zinc(II), d – bis(*N*-ethyl-2-oxy-1-naphathaldiminato)copper(II) (**2**).

These studies have been performed in DMF because it is often used as a solvent for electrochemical measurements. Coordination effects of DMF have been ruled out because its spectra are similar to those taken in dichloromethane, which is a non-coordinating solvent. We conclude that for complexes showing different d–d bands in the solid state and solution spectra (Table 1 and Table 2), different coordination spheres are suggested, but they do not arise as a result of solvent–metal interactions.

The electrochemical study of the complexes was carried out in DMF with Et_4NClO_4 as the supporting electrolyte. The voltammograms were recorded by using a glassy carbon electrode in the +0.1 to –1.6 V (vs. SCE) potential range. The behavior of CuL_2, depicted in Figure 2a, is similar for all copper complexes studied in this work. On the negative scan one well-defined reduction peak is associated with one oxidation peak. The reduction process is diffusion controlled – the cathodic current function ($I_{pc}/v^{1/2}$) is independent of the scan rate (v) (Figure 2b). The peak potential separation is E_p = 80 mV and the ratio of cathodic to anodic peak current is close to unity at low scan rates. All the compounds studied show that the system deviates strongly from reversibility at high sweep rates as shown in Figure 2c. By taking into account Nicholson-Shain criteria, these results are consistent with a quasi-reversible electrochemical process.[14]

Controlled potential electrolysis reveals that a single electron is involved in this reduction step, and therefore the electrochemical reduction response in these complexes reported in Table 3 is consistent with a one electron, diffusion-controlled, quasi-reversible Cu^{II}/Cu^{I} couple. Table 3 also shows electrode kinetic parameters such as the Tafel slope (b), approximately 120 mV/dec^{-1}, obtained from rotating disk electrode (RDE) experiments (Figure 3), elec-

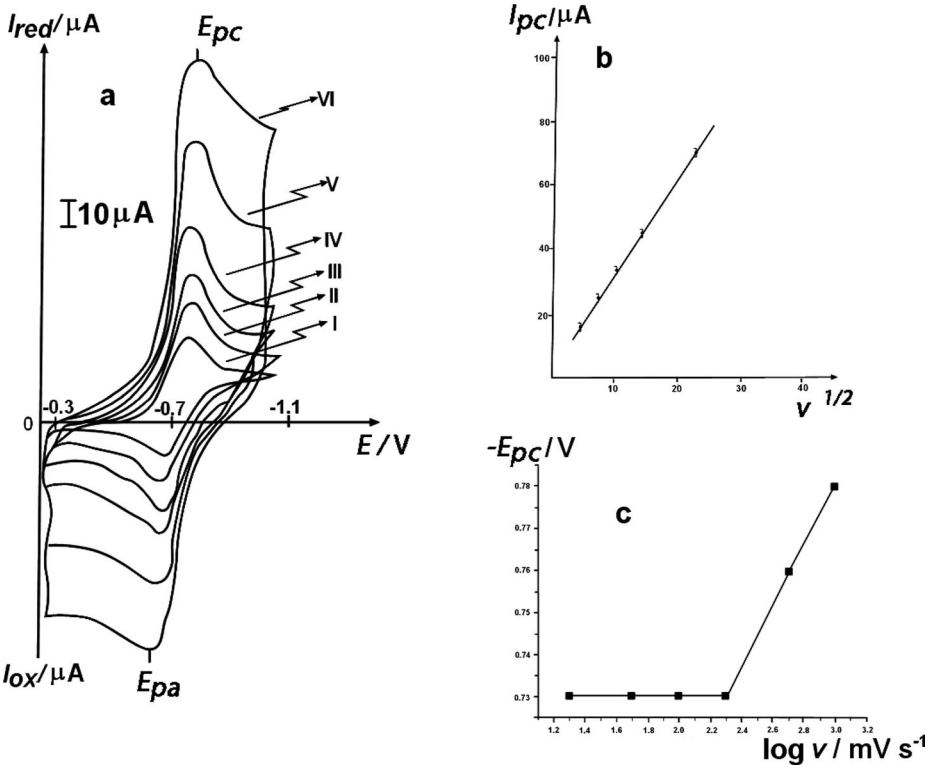

Figure 2. (a) Cyclic voltammetry response of bis(*N*-*tert*-butyl-2-oxy-1-naphthaldiminato)copper(II) (**4**) at different sweep rates: I – 20 mV s^{-1}, II – 50 mV s^{-1}, III – 100 mV s^{-1}, IV – 200 mV s^{-1}, V – 500 mV s^{-1}, VI – 1000 mV s^{-1}. (b) I_{pc} / μA vs. $v^{1/2}$. (c) $-E_{pc}$ vs. log(v / mV s^{-1}).

tronic coefficient transfer (α), between 0.49–0.59, and the heterogeneous rate constant (k_s), ranging from 5.1 to 5.5×10^{-3} cm s^{-1}.[15] These results show that the Cu^{II}/Cu^{I} couple is consistent with a reduction process that has a moderately fast electron transfer, not complicated by side chemical reactions, and whose rate-determining step of the reaction is the electron-transfer process. Therefore, the Cu^{II}/Cu^{I} couple in the complexes studied is a quasi-reversible process in electrochemical terms without significant stereochemical reorganization.

Table 3. Electrochemical parameters for the cathodic reduction of bis(*N*-R-2-oxy-1-naphthaldiminate)copper(II) complexes.

Compound[a]	E_{pc} / V	E_{pa} / V	$E_{1/2}$ / V[b]	b/mV dec^{-1}[c]	α[d]	$k_s \times 10^3$/cm[e]
1	–0.95	–0.87	–0.91	120	0.49	5.1
2	–0.95	–0.87	–0.91	120	0.49	5.1
3	–0.78	–0.7	–0.74	120	0.49	5.5
4	–0.73	–0.65	–0.69	100	0.59	5.5

[a] 1 mM in DMF; 0.1 M TEAP. [b] $E_{1/2}$ values calculated as ½(E_{pc} + E_{pa}) at 0.1 V s^{-1} vs. SCE. [c] Tafel slope (b) obtained from RDE experiments. [d] α = electronic coefficient transfer. [e] Heterogeneous velocity constant (k_s) from CV experiments.[15]

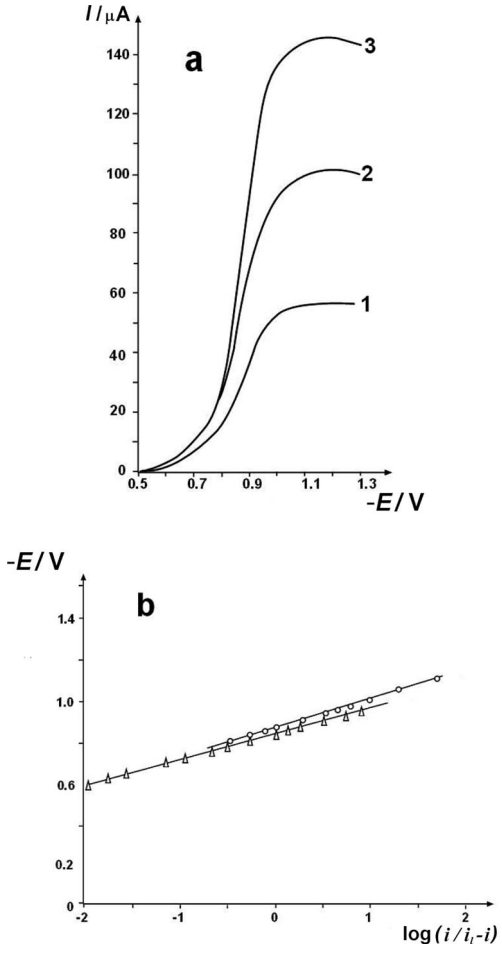

Figure 3. (a) RDE polarization curve for bis(*N*-ethyl-2-oxy-1-naphthaldiminato)copper(II) (**2**) at: 1 – 900 rpm, 2 – 1600 rpm, 3 – 2500 rpm. (b) Tafel plot for **2** (circles) and bis(*N*-isopropyl-2-oxy-1-naphthaldiminato)copper(II) (**3**) (triangles) at ω = 1600 rpm.

Structural Study

Three-dimensional structures of Cu^{II} naphthaldiminates found in the Cambridge Structural Database (CSD) show a large variety in the dihedral angle between the planes N–Cu–O and N′–Cu–O′; *Dih* can be visualized in Scheme 1. Table 4 shows X-ray structural parameters of the title compounds, along with several already known Cu^{II} naphthaldiminates and a few salicylaldiminates, later depicted in Figure 10.

Table 4 shows that bulky R groups induce large *Dih* values. It can be seen that packing effects influence the structural features. Thus, bis[*N*-(cyclooctyl)-2-oxy-1-naphthaldiminato]copper(II) has a bulky c-octyl substituent (c stands for cyclo) that determines a flat-tetrahedral coordination sphere.[17] However, this species has two independent molecules in the asymmetric unit, which show different dihedral angles, *Dih* = 48.1° and 39.6°. Also, for R = adamantyl,[18] there are important packing effects as its Cu^{II} complex crystallizes in two different crystal systems: the triclinic system has a *Dih* of 27.6° and the monoclinic 48.0°. Thus, steric hindrance of the N substituents is not the only factor influencing the coordination sphere in the solid state, as rightly pointed out from EPR data.[17]

Moreover, a small change in the R group can have dramatic structural consequences, as seen in the c-octyl flat-tetrahedral complex mentioned earlier and when both c-octyl groups are replaced by c-heptyl groups and the Cu configuration becomes square-planar (*Dih* = 0°),[19] or better, stepped, since both parallel aromatic rings are generally not coplanar; these results are also reported in Table 4. The stepped arrangement exists for R = c-hexyl[19] and c-butyl,[20] but not for R = c-propyl[20] and c-pentyl,[17] which have flat-tetrahedral coordination spheres (*Dih* = 30.3° and 42.0°, respectively).

In this work, we describe the X-ray structure of bis(*N*-*tert*-butyl-2-oxy-1-naphthaldiminato)copper(II) (**4**), Table 4 and Figure 4. It is less distorted than that of bis(*N*-*tert*-butylsalicylaldiminate)copper(II), according to their *Dih* values of 45.4 and 61.6, respectively. The UV/Vis spectrum is consistent with this flat-tetrahedral arrangement.

In contrast to **4** ,Table 4 shows that R groups having primary C atoms (longer than methyl groups) stabilize a Cu^{II} planar coordination sphere (*Dih* = 0°), which may be associated with the smaller steric hindrance of the primary alkyl moieties. The complex having R = methyl group also has a planar CuN_2O_2 core, but it is unique because it can be: (a) mononuclear when it is[12] or is not[31] intercalated with flat molecules in the crystal, or (b) dinuclear through an additional Jahn–Teller Cu–O bond.[16] Therefore we were interested in studying the copper(II) naphthaldiminate complex having R = ethyl group. The X-ray crystal structure of the ethyl complex **2**, depicted in Figure 5, shows that it is mononuclear and analogous to the corresponding ethyl salicylaldiminate Cu^{II} complex,[16] with *Dih* values of 1.7° and 9.3°, respectively; one wonders why such a difference in distortion, when considering that all other complexes with primary *N*-alkyl substituents have planar Cu^{II} coordination

Table 4. Selected structural parameters for bis(*N*-R-1-oxy-2-naphthaldiminato)copper(II) complexes.[a] X-ray data in the solid state and DFT in the gas phase. (REFCODE: name associated with the corresponding structure in the CSD database)

REFCODE	R	*Dih*[b]	Step[c]	O–Cu–O	N–Cu–N	Cu–O	Cu–N
HENMIW[12]	Met[d]	0	0.13	180	180	1.897, 1.897	1.991, 1.991
MHNAPC03[31]	Met	0	1.10	180	180	1.922, 1.922	1.975, 1.975
AKEVAN[20]	cPr	30.3		158.7	157.9	1.895, 1.904	1.948, 1.954
AKETUF[20]	cBu	0	0.91	180	180	1.896, 1.896	1.992, 1.992
NELWOK[17]	cPen	42.0		149.2	150.8	1.895, 1.879	1.994, 1.989
NUKLEK[19]	cHex	0	0.96	180	180	1.883, 1.883	2.000, 2.000
NELWUW[19]	cHep	0	1.31	180	180	1.899, 1.899	1.900, 1.900
NELXAD[17]	cOct[e]	48.1		146.1	145.0	1.871, 1.894	1.971, 1.972
NELXAD[17]	cOct[e]	39.6		150.3	153.2	1.894, 1.904	1.984, 1.986
KOKCES[18]	Ada[f]	27.6		159.3	161.3	1.895, 1.896	1.979, 1.996
KOKBUH[18]	Ada[g]	48.0		140.0	151.8	1.893, 1.898	1.962, 1.994
LEHCAD[23]	*s*Bu[e]	39.5		149.7	154.4	1.863, 1.887	1.963, 1.065
LEHCAD[23]	*s*Bu[e]	34.8		155.5	154.5	1.877, 1.884	1.925, 1.940
BIPDUA[24]	CHP[h]	0	0.11	180	180	1.832, 1.832	1.913, 1.913
HEPHAM[25]	*n*Oct-ox[i]	0	0.03	180	180	1.887, 1.887	1.995, 1.995
MUGTUD[26]	*i*Pen	25.7		159.5	164.1	1.872, 1.917	1.962, 1.999
QAMFEQ[27]	MeB[j]	28.7		159.0	160.1	1.895, 1.896	1.971, 1.971
QAMGER[27]	Net[k]	38.4		151.0	153.4	1.869, 1.887	1.963, 1.965
VIBNAV[28]	E2ox[l]	6.3		175.8	175.2	1.892, 1.895	1.998, 2.002
MSACOP[23]	Met[a]		0.0	180	180	1.901, 1.901	1.989, 1.989
CUESAL02[16]	Et[a]	9.3		171.0	177.1	1.888, 1.888	2.000, 2.006
ISALCU01[22]	*i*Pr[a]	59.7		137.2	137.9	1.871, 1.884	1.973, 1.982
IPRNCU[21]	*i*Pr	38.3		151.6	153.6	1.892, 1.894	1.965, 1.970
IPONTC[21]	*i*Pr[d]	0	1.41	180	180	1.894, 1.894	1.997, 1.997
X-ray (this work)	*t*Bu	45.4		143.3(1)	152.6(1)	1.906(2), 1.909(2)	1.967(3), 1.966(3)
DFT	*t*Bu	85.9		134.4	149.6	1.988, 1.984	1.999, 1.999
X-ray (this work)	Et	1.7		178.9(1)	178.6(1)	1.893(2), 1.899(2)	1.989(2), 1.993(2)
DFT	Et	38.8		150.5	154.8	1.969, 1.974	1.991, 1.989

[a] Data of Cu^{II} salicylaldiminates plotted in Figure 10. [b] Dihedral angle between the planes N–Cu–O and N′–Cu–O′ in the flat-tetrahedral configuration, Scheme 1. [c] Sum of the distances between the Cu atom and the planes defined by the chelating moieties O–C–C–C–N and O′–C′–C′–C′–N′ in the step configuration. [d] Structures have intercalated molecules. [e] Second molecule in crystal. [f] Adamantyl triclinic crystal. [g] Adamantyl monoclinic crystal. [h] 3-(Cyclohexylamino)propyliminomethyl. [i] *n*-Octyl-2-oxy. [j] α-Methylbenzyl. [k] 1-Naphthyl-ethyl. [l] Ethanol-2-oxy.

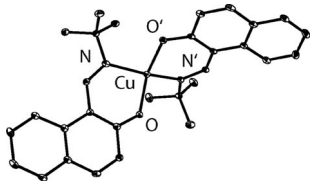

Figure 4. X-ray structure of bis(*N*-*tert*-butyl-2-oxy-1-naphthaldiminato)copper(II) (**4**), showing ellipsoids. Only oxygen, nitrogen and copper atoms are labelled; H atoms are omitted.

spheres in the solid state. The UV/Vis spectrum of **2** in solution suggests it has a planar coordination sphere (Figure 1), which seems to be consistent with the X-ray diffraction results, if one neglects its minor distortion (*Dih* = 1.7°). Therefore, it is apparent that the bulkiness of a small substituent (in this case ethyl) does not necessarily imply a planar coordination sphere in the solid state. We tried to verify the structure of the isolated *N*-ethyl complex **2** by performing DFT geometry minimization and expected to find a planar structure (*Dih* about 0°). The X-ray coordinates were input as starting values in this process, but we did not get a minimum. It was only upon breaking of the stepped planar arrangement, by selecting a *Dih* value greater than 1.7°, that a minimum energy structure was obtained. This flat-tetrahedral arrangement (N–Cu–N′ 154.8°, O–Cu–O 150.5°, *Dih* = 38.8°) is depicted in Figure 6. This configuration is expected to have a similar electronic spectrum as that of the *t*Bu species, but it does not; the question arises: how can the similarity of the solid state and solution state spectra be justified for the *N*-ethyl complex, for a flat-tetrahedral configuration in solution and a "planar" configuration in the solid state? This inconsistency in expected structural geometry between the solid and solution states led to our using DFT methods for an explanation. On the basis of our DFT results, we looked at a possible molecular path of transformation between the minimum depicted in Figure 6 and its equivalent inverted structure. We found a planar centrosymmetric transition state (Figure 7), characterized, as expected, by only one imagi-

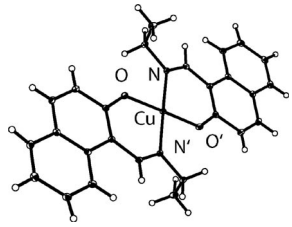

Figure 5. X-ray structure of bis(*N*-ethyl-2-oxy-1-naphthaldiminato)-copper(II) (**2**).

nary frequency, whose energy barrier is 4.4 kcal mol^{-1}, which is easily attainable at room temperature. Therefore, a fluxional complex between both inverted structures, which shows an average symmetric arrangement, accounts for the simpler spectrum of the ethyl complex. This feature would not be possible for **4** because of *t*Bu steric constraints, and so, even in solution, this complex remains nonsymmetric.

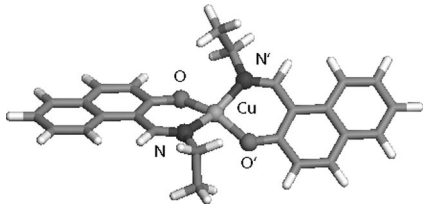

Figure 6. DFT minimum energy structure for bis(*N*-ethyl-2-oxy-1-naphthaldiminato)copper(II) (**2**).

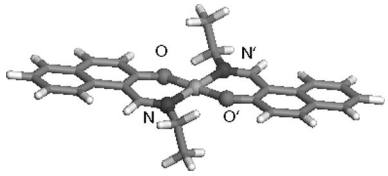

Figure 7. Transition state for the fluxional bis(*N*-ethyl-2-oxy-1-naphthaldiminato)copper(II) complex in solution (**2**).

Spectroscopic information for the complex with a secondary substituent, *i*Pr, is similar to the data for the *N*-ethyl complex in solution, and the complexes should be expected to have similar fluxional behavior.

Since, in solution, the *N*-ethyl flat-tetrahedral arrangement may be a result of steric hindrance between the ethyl group and the oxygen atom facing it, we also optimized the geometry of the mononuclear methyl complex **1** using DFT and found a similar result to that of the *N*-ethyl derivative **2**, Figure 8. Relative to the ethyl complex **2**, the methyl complex **1** is less bulky, and the resulting distortion is consequently smaller, as shown by the N–Cu–N′ (158.3°) and O–Cu–O′ (157.7°) bond angles and the dihedral angle (28.9°). The corresponding energy barrier (1.1 kcal mol^{-1}) is smaller for **1** than that of the ethyl complex **2**, as expected. In contrast, a potential complex with R = H is planar, as seen in Figure 9, because of no hindrance caused by the H atom. Exact values of 180° for N–Cu–N′ and O–Cu–O′ were imposed by *C*2*h* symmetry in the geometry optimization process that converged, which shows no imaginary frequency, as expected for a minimum of energy. We conclude that steric effects in solution distort the naphthaldiminate *N*-ethyl complex from planarity, and small energies are at play in solution that allow a fluxional and continuous transformation of the flat-tetrahedral complex. This behavior is forbidden for the bulky *t*Bu substituent in **4** because of its greater hindrance.

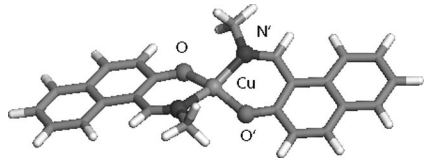

Figure 8. DFT minimum energy structure for bis(*N*-methyl-2-oxy-1-naphthaldiminato)copper(II) (**1**).

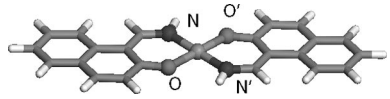

Figure 9. DFT minimum energy structure for bis(*N*-H-2-oxy-1-naphthaldiminato)copper(II).

The DFT results obtained in this study should be considered as an indication that the structures can be different in solution from those in the solid state, not as a proof for that.

Conclusions

Bis(*N*-alkyl-2-oxy-1-naphthaldiminato)copper(II) structures are compared in the solid state and in DMF solutions, by using electronic spectroscopy, X-ray diffraction, DFT calculations, and cyclic voltammetry. There is an important role played by crystallographic packing forces: certain structural molecular features such as distortion in the solid state differ markedly when these compounds are dissolved in DMF or dichloromethane. There is also a low energy barrier in solution for a fluxional flat-tetrahedral configuration of the ethyl complex **2**. This type of flat-tetrahedral arrangement is easily overruled by packing forces in the crystal, which make it appear as planar; other primary *N*-alkyl complexes reported in the literature may behave similarly. A potential driving force may be associated with this phenomenon as the primary *N*-alkyl chains tend to establish a typical paraffinic interaction in the crystal.

In addition, correlations exist between the solid state geometry and the Cu^{II}/Cu^{I} redox potentials, which also apply to the equivalent copper(II) salicylaldiminates, although the absolute values are not strictly coincident, as shown in Figure 10.

From Table 3, it can be seen that E_{pc} for the Cu^{II}/Cu^{I} couple in bis(*N*-R-oxy-naphthaldiminato)copper(II) complexes shifts to more anodic values by ca. 220 mV as the N substituent in the Schiff base ligand is changed from methyl to *t*Bu. Therefore, the bulky *t*Bu group forces a square-planar distortion and tunes the redox potential of the Cu^{II}/Cu^{I} couple to stabilize the Cu^{I} species, i.e. with the *t*Bu complex (*Dih* = 85.9°), which has a more tetrahedral geometry than the ethyl derivative (*Dih* = 38.8°), the former is reduced more easily than the latter, as the expected *Dih* value for a perfect tetrahedron (90°) is closer to the value in the *t*Bu Cu^{II} complex. Thus, when correlating the dihedral angle (Table 4) with the respective redox potentials (Table 3), a general increase in the reduction potentials of

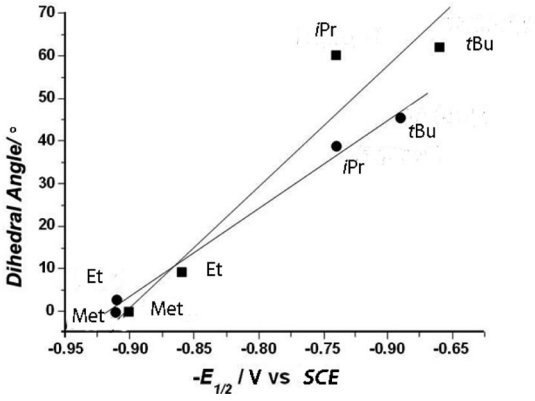

Figure 10. Influence of the dihedral angle on the Cu^{II}/Cu^{I} redox couple for bis(*N*-alkyl-2-oxy-1-naphthaldiminato)copper(II) complexes (circles). Data for bis(*N*-alkyl-2-oxy-1-salicylaldiminato)copper(II) complexes are included for comparison (squares).[2a]

ca. 4.7 mV per degree is observed as the geometry moves from planar to tetrahedral. For the salicylaldiminate copper(II) complexes, a similar behavior is observed, but the distortion from planarity is greater when the same alkyl substituent is linked to the imine nitrogen atom; specific ligand electronic features were associated with this phenomenon.[19] Since the DFT studies found a fluxional flat-tetrahedral behavior in solution, a more accurate correlation will be described in a following publication.

Experimental Section

Synthesis of Copper(II) Complexes: The bis(2-hydroxy-1-naphthaldehydate)copper(II) complex and the respective amines, H_2NR (R = methyl, ethyl, *i*Pr, and *t*Bu), were heated at reflux in ethanol following reported procedures.[25,32–35] Solid bis(*N*-R-2-oxy-1-naphthaldiminato)copper(II) complexes were obtained after filtering, washing with hot ethanol, and drying for 6 h in an oven. Recrystallization from chloroform gave ca. 80% yield in all cases.

Bis(*N*-methyl-2-oxy-1-naphthaldiminato)copper(II) (1): Brown solid, m.p. 233 °C. FTIR (KBr): $\nu_{(C=N)}$ = 1615, $\nu_{(C-O)}$ = 1360, $\nu_{(Cu-N)}$ = 640 cm^{-1}. $C_{24}H_{20}CuN_2O_2$ (431.97): calcd. C 65.03, H 4.50, N 6.50; found C 65.70, H 4.60, N 6.40.

Bis(*N*-ethyl-2-oxy-1-naphthaldiminato)copper(II) (2): Green solid, m.p. 220 °C. FTIR (KBr): $\nu_{(C=N)}$ = 1610, $\nu_{(C-O)}$ = 1365, $\nu_{(Cu-N)}$, = 644 cm^{-1}. $C_{26}H_{24}CuN_2O_2$ (460.03): calcd. C 67.80, H 5.25, N 6.00; found C 67.40, H 5.00, N 5.70.

Bis(*N*-isopropyl-2-oxy-1-naphthaldiminato)copper(II) (3): Brown solid, m.p. 197 °C. FTIR (KBr): $\nu_{(C=N)}$ = 1610, $\nu_{(C-O)}$ = 1360, $\nu_{(Cu-N)}$ = 640 cm^{-1}. $C_{28}H_{28}CuN_2O_2$ (488.08): calcd. C 69.47, H 5.73, N 5.73; found C 69.90, H 5.80, N 5.70.

Bis(*N*-*tert*-butyl-2-oxy-1-naphthaldiminato)copper(II) (4): Brown solid, m.p. 202 °C. FTIR (KBr): $\nu_{(C=N)}$ = 1610, $\nu_{(C-O)}$ = 1360, $\nu_{(Cu-N)}$ = 640 cm^{-1}. $C_{30}H_{32}CuN_2O_2$ (516.14): C 69.81, H 6.25, N 5.43; found C 69.90, H 6.00, N 6.00.

Bis(*N*-isopropyl-2-oxy-1-naphthaldiminato)zinc(II) (5): This compound was synthesized following the method reported in the literature.[13] UV/Vis spectra were recorded by using a Carl Zeiss DMR-22 spectrometer and Nujol mulls on Whatman paper No. 52 for solids and *N*,*N*-dimethylformamide (DMF) solvent for solutions. Voltammograms were recorded by using a potentiostat/galvanostat PAR 173, universal programmer PAR 175, and a digital coulometer PAR 179 from Princeton Applied Research. An H cell with three electrodes, namely glassy carbon, platinum, and saturated calomel electrode (SCE) as working, auxiliary, and reference electrode, respectively, was used. Tetraethylammonium perchlorate, was used as the supporting electrolyte and DMF as solvent. All measurements were carried out under a nitrogen atmosphere. Suitable crystals for X-ray diffraction data were obtained by dissolving the samples in a mixture of 1:1 dichloromethane/ethanol solutions and on standing in a refrigerator for a week. Data for **4** and **2** were col-

Table 5. X-ray data of bis(*N*-*tert*-butyl-2-oxy-1-naphthaldiminato)copper(II) and bis(*N*-ethyl-2-oxy-1-naphthaldiminato)copper(II).

	4	**2**
Empirical formula	$C_{30}H_{32}CuN_2O_2$	$C_{26}H_{24}CuN_2O_2$
Formula weight	516.12	460.02
Temperature / K	125(2)	125(2)
Wavelength / Å	0.71073	0.71073
Crystal system, space group	orthorhombic, $P2_12_12$	monoclinic, $P2_1$
a / Å	14.2467(12)	5.6309(3)
b / Å	16.1222(13)	16.6252(8)
c / Å	11.1325(9)	10.9817(6)
β / °	–	92.982(1)
Volume / $Å^3$	2557.0(4)	1026.66(9)
Z	4	2
Density / mg mm^{-3}	1.341	1.488
Absorption coefficient	0.884	1.091
Crystal size / mm	0.34 × 0.14 × 0.05	0.33 × 0.06 × 0.06
θ range data collection	1.83, 24.75	1.86, 30.48
Limiting indices	–16, 16/–18, 18/–13, 13	–8, 7/–23, 23/–15, 15
Data collected/unique	25380/4385	14601/5788
Flack parameter	0.010(15)	0.244(9)
Max, min. transmission	0.94, 0.85	0.94, 0.71
Refinement method	F^2	F^2
Refined data/parameters	3495/322	5238/354
Goodness-of-fit on F^2	1.067	1.041
Final *R*, R_w [$I > 2\sigma(I)$]	0.0377, 0.0743	0.0309/0.0685
Largest diff. peak, hole / e $Å^{-3}$	0.489, –0.410	0.463, –0.309

lected at 125 K by using a Bruker SMART APEX II CCD X-ray diffractometer. Structure resolution and refinement were performed with ShelX;[36] details are included in Table 5. Those H atoms not found in Fourier maps were included from models and constrained as riding on their bound atoms. The theoretical study involved calculations by using software programs from Accelrys.[37] Density functional theory code DMol3 was applied to calculate energies (see below), implemented in Materials Studio 4.4 (PC platform).[38] We employed the double numerical polarized (DNP) basis set that includes all the occupied atomic orbitals plus a second set of valence atomic orbitals, and polarized d-valence orbitals,[39] and correlation generalized gradient approximation (GGA) was applied in the manner suggested by Perdew–Burke–Ernzerhof (PBE);[40] these are the conditions for the highest-accuracy level in DMol3. The spin unrestricted approach was exploited in which all electrons are considered explicitly. The real space cutoff of 5 Å was imposed for numerical integration of the Hamiltonian matrix elements. The self-consistent-field convergence criterion was set to the root-mean-square change in the electronic density to be less than 10^{-6} electron $Å^{-3}$. The convergence criteria applied during geometry optimization were 2.72×10^{-4} eV for energy and 0.054 eV $Å^{-1}$ for force.

CCDC-725454 (**2**) and -725455 (**4**) contain the supplementary crystallographic data for this paper. These data can be obtained free of charge from The Cambridge Crystallographic Data Centre via www.ccdc.cam.ac.uk/data_request/cif.

Acknowledgments

M. V., J. Z., and J. C. acknowledge support from the Comision Nacional de Ciencia y Tecnología (CONICYT) project No. 1060030; M. V. and J. C. acknowledge support from the Dirección de Investigaciones Cientificas y Tecnologicas, Universidad de Santiago de Chile (DICYT, USACH), project No. 020743CM. The US National Science Foundation is thanked, through the grant 0521237, for the X-ray diffractometer.

[1] a) Y. Wang, T. D. P. Stack, *J. Am. Chem. Soc.* **1996**, *118*, 13097–13098; b) Y. Wang, J. L. Dubois, B. Hedman, K. O. Hodgson, T. D. P. Stack, *Science* **1998**, *279*, 537–540.
[2] a) G. S. Patterson, R. H. Holm, *Bioinorg. Chem.* **1975**, *4*, 257–275; b) H. Yokoi, A. W. Addison, *Inorg. Chem.* **1977**, *16*, 1341–1349; c) J. Costamagna, J. Vargas, R. Latorre, A. Alvarado, G. Mena, *Coord. Chem. Rev.* **1992**, *119*, 67–88.
[3] C. E. Dahm, D. G. Peters, *Anal. Chem.* **1994**, *66*, 3117–3123.
[4] D. Chartterjee, A. Mitra, *J. Mol. Catal. A* **1999**, *144*, 363–367.
[5] P. Kuo, K. Wong, *Electrochem. Commun.* **1999**, *1*, 559–561.
[6] A. T. Chaviara, P. C. Christidis, A. Papageorgiou, E. Chryselou, D. J. Hadjipavlou, C. A. Bolos, *J. Inorg. Biochem.* **2005**, *99*, 2102–2109.
[7] C. Ji, S. E. Day, W. C. Silvers, *J. Electroanal. Chem.* **2008**, *622*, 15–21.
[8] J. Costamagna, F. Caruso, J. Vargas, V. Manríquez, *Inorg. Chim. Acta* **1998**, *267*, 151–158.
[9] a) M. K. Taylor, J. Reglinski, L. E. A. Berlouis, A. R. Kennedy, *Inorg. Chim. Acta* **2006**, *359*, 2455–2464; b) M. K. Taylor, K. D. Trotter, J. Reglinski, L. E. A. Berlouis, A. R. Kennedy, C. M. Spickett, R. J. Sowden, *Inorg. Chim. Acta* **2008**, *361*, 2851–2862; c) M. K. Taylor, D. E. Stevenson, L. E. A. Berlouis, A. R. Kennedy, J. Reglinski, *J. Inorg. Biochem.* **2006**, *100*, 250–259.
[10] A. B. Lever, *Inorganic Electronic Spectroscopy*, Elsevier, Amsterdam, pp. 355–361, **1968**.
[11] L. Araya, J. Vargas, J. Costamagna, *Trans. Met. Chem.* **1986**, *11*, 312–316.
[12] M. Shiotsuka, Y. Okaue, N. Matsumoto, H. Okawa, T. Isobe, *J. Chem. Soc., Dalton Trans.* **1994**, 2065–2070.
[13] T. Yu, W. Su, W. Li, Z. Hong, R. Hua, B. Li, *Thin Solid Films* **2007**, *515*, 4080–4084.
[14] R. S. Nicholson, I. Shain, *Anal. Chem.* **1964**, *33*, 706–723.
[15] R. P. Baldwin, K. Ravichandran, R. K. Johnson, *J. Chem. Educ.* **1984**, *61*, 820–823.
[16] G. R. Clark, J. M. Waters, T. N. Waters, G. J. Williams, *J. Inorg. Nucl. Chem.* **1977**, *39*, 1971–1975.
[17] M. Aguilar-Martinez, R. Saloma-Aguilar, N. Macias-Ruvalcaba, R. Cetina-Rosado, A. Navarrete-Vazquez, V. Gomez-Vidales, A. Zentella-Dehesa, R. A. Toscano, S. Hernandez-Ortega, J. M. Fernandez-G, *J. Chem. Soc., Dalton Trans.* **2001**, 2346–2352.
[18] E. Acevedo-Arauz, J. M. Fernandez-G., M. J. Rosales-Hoz, R. A. Toscano, *Acta Crystallogr., Sect. C* **1992**, *48*, 115–120.
[19] J. M. Fernandez-G, M. R. Patino-Maya, R. A. Toscano, L. Velasco, M. Otero-Lopez, M. Aguilar-Martinez, *Polyhedron* **1997**, *16*, 4371–4378.
[20] I. Castillo, J. M. Fernandez-Gonzalez, J. L. Garate-Morales, *J. Mol. Struct.* **2003**, *657*, 25–35.
[21] N. Matsumoto, Y. Nonaka, S. Kida, S. Kawano, I. Ueda, *Inorg. Chim. Acta* **1979**, *37*, 27–36.
[22] R. J. Butcher, E. Sinn, *Inorg. Chem.* **1976**, *15*, 1604–1608.
[23] J. M. Fernandez-G., P. Tepal-Sanchez, S. Hernandez-Ortega, *J. Mol. Struct.* **2006**, *787*, 1–7.
[24] P. Zhang, *Acta Crystallogr., Sect. E* **2004**, *60*, 1808–1810.
[25] A. Rios-Escudero, M. Villagrán, F. Caruso, J. P. Muena, E. Spodine, D. Venegas-Yazigi, L. Massa, L. J. Todaro, J. H. Zagal, M. Paez, J. Costamagna, *Inorg. Chim. Acta* **2006**, *359*, 3947–3953.
[26] J. M. Fernandez-G, F. A. Lopez-Duran, S. Hernandez-Ortega, V. Gomez-Vidales, N. Macias-Ruvalcaba, M. Aguilar-Martinez, *J. Mol. Struct.* **2002**, *612*, 69–79.
[27] A. L. Iglesias, G. Aguirre, R. Somanathan, M. Parra-Hake, *Polyhedron* **2004**, *23*, 3051–3062.
[28] W. Maniukiewicz, M. Bukowska-Strzyzewska, *J. Crystallogr. Spectrosc. Res.* **1990**, *20*, 363–369.
[29] E. C. Lingafelter, G. L. Simmons, B. Morosin, C. Scheringer, C. Freiburg, *Acta Crystallogr.* **1961**, *14*, 1222–1225.
[30] E. E. Castellano, O. J. R. Hodder, C. K. Prout, P. J. Sadler, *J. Chem. Soc. A* **1971**, 2620–2627.
[31] G. R. Clark, J. M. Waters, T. N. Waters, G. J. Williams, *J. Inorg. Nucl. Chem.* **1975**, *37*, 2455–2458.
[32] A. Chakravorty, R. H. Holm, *Inorg. Chem.* **1964**, *3*, 1010–1015.
[33] N. Matsumoto, T. Hara, A. Hirano, A. Ohyoshi, *Bull. Chem. Soc. Jpn.* **1983**, *56*, 2727–2732.
[34] J. Costamagna, N. P. Barroso, B. Matsuhiro, M. Villagran, *Inorg. Chim. Acta* **1998**, *273*, 191–195.
[35] J. Costamagna, L. E. Lillo, B. Matsuhiro, M. D. Noseda, M. Villagrán, *Carbohydr. Res.* **2003**, *338*, 1535–1542.
[36] ShelX: G. M. Sheldrick, *Acta Crystallogr., Sect. A* **2008**, *64*, 112–122.
[37] Accelrys Inc., 10188 Telesis Court, Suite 100 San Diego, CA 92121, USA.
[38] B. Delley, *J. Chem. Phys.* **2000**, *113*, 7756–7764.
[39] J. P. Perdew, J. A. Chevary, S. H. Vosko, K. A. Jackson, M. R. Pederson, D. J. Singh, C. Fiolhais, *Phys. Rev. B: Cond. Mater. Mater. Phys.* **1992**, *46*, 6671–6687.
[40] A. D. Becke, *Phys. Rev.* **1988**, *A38*, 3098–3100.

Received: March 31, 2009
Revised Version Received: January 9, 2010
Published Online: February 12, 2010

